Journal of Visualized Experiments

Synthesis of pH Dependent Pyrazole, Imidazole, and Isoindolone Dipyrrinone Fluorophores Using a Claisen-Schmidt Condensation Approach

--Manuscript Draft--

Article Type:	Invited Methods Article - Author Produced Video
Manuscript Number:	JoVE61944R2
Full Title:	Synthesis of pH Dependent Pyrazole, Imidazole, and Isoindolone Dipyrrinone Fluorophores Using a Claisen-Schmidt Condensation Approach
Corresponding Author:	Zachary Woydziak Nevada State College Henderson , Nevada UNITED STATES
Corresponding Author's Institution:	Nevada State College
Corresponding Author E-Mail:	Zachary.Woydziak@nsc.edu
Order of Authors:	Zachary Woydziak
	Nicole Benson
	Adam Davis
Additional Information:	
Question	**Response**
Please indicate whether this article will be Standard Access or Open Access.	Standard Access (US$1200)
Please confirm that you have read and agree to the terms and conditions of the author license agreement that applies below:	I agree to the Author License Agreement
Please specify the section of the submitted manuscript.	Chemistry
Please indicate whether this article will be Standard Access or Open Access.	Standard Access ($1400)
Please provide any comments to the journal here.	

TITLE:

Synthesis of pH Dependent Pyrazole, Imidazole, and Isoindolone Dipyrrinone Fluorophores Using a Claisen-Schmidt Condensation Approach

AUTHORS AND AFFILIATIONS:

Nicole Benson[1], Adam Davis[2], Zachary R. Woydziak[1]

1. Department of Physical and Life Sciences, Nevada State College, Henderson, NV
2. Department of Humanities, Nevada State College, Henderson, NV

Corresponding Author:
Zachary R. Woydziak
zachary.woydziak@nsc.edu

Email Addresses of Co-authors:
Nicole Benson (nicole.benson@nsc.edu)
Adam Davis (adam.davis@nsc.edu)

KEYWORDS:

Claisen-Schmidt Condensation, Photoisomerization, pH dependent fluorescence, fluorophore, dipyrrinone, pyrazole, imidazole, and isoindolone

SUMMARY:

The Claisen-Schmidt condensation reaction is an important methodology for the generation of methine-bridged conjugated bicyclic aromatic compounds. Through utilizing a base-mediated variant of the aldol reaction, a range of fluorescent and/or biologically relevant molecules can be accessed through a generally inexpensive and operationally simple synthetic approach.

ABSTRACT:

Methine-bridged conjugated bicyclic aromatic compounds are common constituents of a range of biologically relevant molecules such as porphyrins, dipyrrinones, and pharmaceuticals. Additionally, restricted rotation of these systems often results in highly to moderately fluorescent systems as observed in 3H,5H-dipyrrolo[1,2-c:2',1'-f]pyrimidin-3-ones, xanthoglows, pyrroloindolizinedione analogs, BODIPY analogs, and the phenolic and imidazolinone ring systems of Green Fluorescent Protein (GFP). This manuscript describes an inexpensive and operationally simple method of performing a Claisen-Schmidt condensation to generate a series of fluorescent pH dependent pyrazole/imidazole/isoindolone dipyrrinone analogs. While the methodology illustrates the synthesis of dipyrrinone analogs, it can be translated to produce a wide range of conjugated bicyclic aromatic compounds. The Claisen-Schmidt condensation reaction utilized in this method is limited in scope to nucleophiles and electrophiles that are enolizable under basic conditions (nucleophile component) and non-enolizable aldehydes (electrophile component). Additionally, both the nucleophilic and electrophilic reactants must contain functional groups that will not inadvertently react with hydroxide. Despite these limitations, this methodology offers access to completely novel systems that can be employed as

biological or molecular probes.

INTRODUCTION:

A number of conjugated bicyclic systems, in which two aromatic rings are linked by a monomethine bridge, undergo isomerization via bond rotation, when excited with a photon (**Figure 1A**)[1-5]. The excited isomer will generally relax to the ground state through non-radiative decay processes[6]. If the energy barrier to bond rotation is increased to a large enough extent, it is possible to restrict or prevent the photoisomerization. Instead, photonic excitation results in an excited singlet state that often relaxes via fluorescence rather than non-radiative decay (**Figure 1B**). Restraining photoisomerization is most commonly accomplished by mechanically restricting bond rotation through tethering the two aromatic ring systems by covalent linkages, thereby locking the molecule into a particular isomeric state. This approach has been utilized to create several different fluorescent tricyclic dipyrrinone and dipyrrolemethane analogs such as: 3H,5H-dipyrrolo[1,2-c:2',1'-f]pyrimidin-3-ones (**1**), xanthoglows (**2**)[6,7], pyrroloindolizinedione analogs (**3**)[8], and BODIPY analogs[9] (**4**, **Figure 2**) whereby the pyrrolidine and/or pyrrole ring systems are tethered with methylene, carbonyl, or boron difluoro linkers. Typically, 1-4 possess $\Phi_F > 0.7$ suggesting these systems are very efficient as fluorophore units.

It is also possible to restrict photoisomerization through means other than covalently linking the ring systems. For example, the phenolic and imidazolinone rings (**Figure 2**) of Green Fluorescent Protein (GFP) are restricted to rotation by the protein environment; the restrictive setting increases the quantum yield by three orders of magnitude in comparison to the same chromophore unit in free solution[10]. It is believed that the protein scaffold of GFP provides a rotational barrier through steric and electrostatic effects[11]. Recently, our group in collaboration with the Odoh group at the University of Nevada, Reno discovered another fluorophore system that bears structural similarity to the dipyrrinone-based xanthoglow systems (**Figure 2**)[12]. These dipyrrinone analogs, however, differ from the xanthoglow system in that intramolecular hydrogen bonds, rather than covalent bonds, deter photoisomerization and result in a fluorescent bicyclic system. Furthermore, the pyrazole, imidazole, and isoindolone dipyrrinone analogs can hydrogen bond in protonated and deprotonated states; deprotonation results in the red-shifting of both the excitation and emission wavelengths, likely due to a change in the electronic nature of the system. While hydrogen bonding has been reported to increase quantum yields though restricted rotation[13-16], we are unaware of any other fluorophore system in which restricted isomerization serves as a mode of fluorescence in both protonated and deprotonated states of the molecule. Therefore, these pH dependent dipyrrinone fluorophores are unique in that respect.

In this video, we focus on the synthesis and chemical characterization of the fluorescent dipyrrinone analog series. In particular, there is an emphasis placed on the Claisen-Schmidt condensation methodology that was used to construct the complete series of fluorescent analogs. This reaction relies on the generation of a base-mediated vinylogous enolate ion which attacks an aldehyde group, to produce an alcohol that subsequently undergoes elimination. For the dipyrrinone analog series, a pyrrolinone/isoindolone is converted to an enolate to facilitate an attack upon an aldehyde group attached to a pyrazole or imidazole ring (**Figure 3**); after

elimination a fully conjugated bicyclic system, linked by a methine-bridge, is formed. It is noteworthy that the entire series of dipyrrinone analogs can be constructed from readily available commercial materials and can be produced in a single one-pot reaction sequence typically in moderate to high yields (yields range from approximately 50-95%). Since most of the dipyrrinone analogs are highly crystalline in nature, very little purification outside of standard workup conditions is required to produce analytically pure samples. Consequently, this fluorophore system requires only a few steps to access from readily available commercial materials and can be synthesized, purified, and prepared for analytical or biological studies in a relatively short time frame.

PROTOCOL:

1. General Procedure for Synthesis of Dipyrrinone Analogs 16 – 25

1.1. Dissolve pyrrolinone/isoindolone (1.00 mmol) and the corresponding pyrazole/imidazole aldehyde (1.00 mmol) in 5.0 mL of ethanol in a round-bottom flask.

1.2. Add aqueous KOH (24.0 mmol, 10 M, 2.40 mL) to the flask in one portion.

1.3. Stir and reflux the mixture until reaction completion is confirmed by TLC (See **Table 1** for a list of reaction times). A TLC eluent of 10% methanol in dichloromethane was used and the analogs have been observed to possess R_f values in or around the range of 0.62 to 0.86. Apply a sufficient amount of vacuum grease or use a PTFE sleeve at the interphase of glass joints to prevent the glass of the condenser and the round-bottom flask from seizing under high temperatures and basic conditions.

1.4. Allow the reaction mixture to cool to room temperature and evaporate volatiles under reduced pressure using a rotary evaporator.

1.5. Cool the reaction mixture to 0 °C using an ice bath.

1.6. Neutralize the remaining oily mixture by adding acetic acid (30.0 mmol, 1.70 mL) in one portion.

1.7. Purify the resulting product material using vacuum filtration (see **Step 2a**, for compounds: **17**, **18**, **20** – **22**, **24** and **25**) or use liquid-liquid extraction/column chromatography (see **Step 2b**, for compounds: **16**, **19**, and **23**).

2. Procedure Purification

2.1. via Vacuum Filtration

2.1.1. Fit a Hirsch funnel to a side-arm flask using a fitted rubber adapter.

2.1.2. Apply a piece of round filter paper to the Hirsch funnel and lightly wet using deionized water to allow adherence to the funnel.

2.1.3. Connect a vacuum source to the side-arm of the flask and ensure that there is a sufficient vacuum seal by making sure none of the glassware can be pulled apart while under vacuum.

2.1.4. Pour the flask containing the crystallized product over the vacuum filter and allow to filter. Rinse the crystals with 10 mL of ice-cold deionized water.

2.1.5. Allow the filtered crystals to continue to dry on top of the filter paper, while still connected to the vacuum source, following the filtration of all liquids.

2.1.6. Collect the filtered crystals and place in a 25 mL round-bottom flask.

2.1.7. Attach the round-bottom flask to a fritted ground glass joint/vacuum line adapter. Secure the glass joint union with a keck clip.

2.1.8. To the ribbed end of the glass high vacuum line adapter, attach a vacuum line that is routed to a high vacuum pump and adequately cool a vacuum trap (using coolant such as liquid nitrogen or dry ice/acetone) to condense any volatile materials that may evaporate from the crystalline material. Turn on the high vacuum pump to ensure complete evaporation of any trace amounts of remaining solvent from the crystals.

2.1.9. Allow the crystals to dry under high vacuum for a minimum of 1 h. Remove the round-bottom flask from the vacuum line/adapter, turn off the high vacuum pump, and clean out the vacuum trap.

2.2. Procedure Purification via Column Chromatography

2.2.1. Dilute the acetic acid treated reaction mixture contents (from step 1.6) with 10 mL of deionized water and transfer into a separatory funnel. Add 10 mL of dichloromethane to the separatory funnel. Gently shake and vent the separatory funnel in order to separate the two layers.

2.2.2. Extract the aqueous layer using subsequent portions of dichloromethane (3 x 5 mL). Combine the organic fractions and dry using anhydrous Na_2SO_4. Decant and remove all volatiles under reduced pressure using a rotary evaporator.

2.2.3. Dilute the residue obtained from step 2.2.2. with 5 mL of CH_2Cl_2. Perform flash column chromatography using approximately 75 g of silica gel. Elute the sample with a solution of 10% methanol in dichloromethane.

2.2.4. Remove the collected fractions of solvent under reduced pressure using a rotary evaporator. Transfer the solid residue to a 25 mL round-bottom flask using approximately 10 mL of CH_2Cl_2. Remove the solvent under reduced pressure using a rotary evaporator.

2.2.5. Dry the remaining solid residue under high vacuum as previously described in steps 2.1.7 – 2.1.9.

3. Molar Absorptivity Acquisition and UV/Vis pK_a Studies for Analogs 16 – 25

3.1. Create compound stock solutions for UV/Vis Spectrophotometry for analogs **16 – 25**.

3.1.1. Weigh out 10 μmol of the selected dipyrrinone analog (**16 – 25**) and add it to a 10 mL volumetric flask.

3.1.2. 3.1.2 Add DMSO to the 10.0 mL mark on the volumetric flask.

NOTE: If the compound does not dissolve entirely, heat the flask using a heat gun and agitate the flask as needed to completely dissolve the compound.

3.2. Make phosphate buffered saline (PBS) solutions at various pH levels. The analogs were characterized in PBS buffers ranging in pH from approximately 4 to 15.

3.2.1. Using a 1 L volumetric cylinder, create 1 L of PBS stock solution by diluting 100 mL of PBS (x100) in 900 mL of deionized water.

3.2.2. Transfer 50 mL of the prepared PBS stock solution (step 3.2.1) to a 100 mL beaker and add a magnetic stir bar. Then using a calibrated pH meter to monitor changes in pH, titrate the PBS buffer with either aqueous 1.0 M NaOH (to obtain buffers with pH > 7.0) or 1.0 M HCl (to obtain buffers with pH < 7.0).

NOTE: To obtain data that results in a well-defined titration curve, we recommend generating pH buffers in increments of 0.1 pH units within ± 0.5 of the anticipated point of inflection and increments of 0.5 outside of the anticipated point of inflection.

3.3. Acquire molar absorptivity spectra for analogs **16 – 25** in PBS (pH 7.0) and 1.0 M NaOH (pH 14.0) solutions.

3.3.1. Prepare a “blank” using a clean and dry quartz cuvette then add 2.0 mL of either PBS stock solution (pH 7.0) or aqueous 1.0 M NaOH to the cuvette using a 100 – 1000 μL micropipette.

NOTE: It is important to the integrity of the blank solution data acquisition process to ensure that there are no air bubbles in the cuvette solution and to thoroughly wipe the sides of the cuvette with a Kim wipe to prevent light scattering resulting from dust or debris on the outside of the

cuvette. If bubbles persist, gently and repeatedly tap the cuvette on a paper towel laid on a hard surface.

3.3.2. Using a UV/Vis spectrophotometer, blank the selected solution for a 200 - 800 nm range.

3.3.3. Into a second clean and dry quartz cuvette add 2.00 mL of either PBS (pH 7.0) or 1.0 M NaOH (pH 14) followed by 10 µL of the dipyrrinone analog (**16 – 25**) stock solution (see step 3.1) with a 5-50 µL micropipette. Place a cap on the cuvette and shake well in addition to inverting the cuvette.

NOTE: It is important to the integrity of the sample solution data acquisition process to ensure that there are no air bubbles in the cuvette solution and to thoroughly wipe the sides of the cuvette with a Kim wipe to prevent light scattering resulting from dust or debris on the outside of the cuvette. If bubbles persist, gently and repeatedly tap the cuvette on a paper towel laid on a hard surface.

3.3.4. Using the UV/Vis spectrophotometer, acquire an absorption spectrum for the dipyrrinone analog solution for a 200 - 800 nm range.

3.3.5. To the same cuvette, add an additional 10 µL of the dipyrrinone analog stock solution and repeat steps 3.3.3 and 3.3.4.

3.3.6. Repeat step 3.3.5 until a total of 50 µL of dipyrrinone analog stock solution has been added to the cuvette in order to acquire at least five excitation wavelength data points. Repeat steps 3.3.1 – 3.3.6 until all stock solutions of **16** - **25** have been obtained in both PBS (pH 7.0) and 1.0 M NaOH.

3.4. Obtain molar absorptivity values for **16** - **25** in PBS (pH 7.0) and 1.0 M NaOH using best fit linear regression analysis.

3.4.1. Using a graphing program such as GraphPad Prism 7, plot the measured absorbance (y-axis) against the dipyrrinone analog concentration (x-axis). Create a best-fit linear regression analysis for the five plotted points. A linear relationship should be observed and statistical analysis should show an R^2 value ≥ 0.98.

3.4.2. Repeat step 3.4.1 for analogs **16 – 25** in PBS (pH 7.0) and 1.0 M NaOH.

3.4.3. Calculate the molar absorptivity for **16 – 25** in PBS (pH 7.0) and 1.0 M NaOH using the extrapolated slope value from the best fit linear curve.

3.5. Determine the pK_a values of **16 – 25**: Studies Using UV/Vis Spectrophotometry

3.5.1. Into a clean and dry quartz cuvette, transfer 1,900 µL of the PBS buffer at the selected pH level (prepared in Step 3.2) using a 100 – 1000 µL micropipette.

NOTE: We have noticed upon storage that a white precipitate can form in some of the buffers. To ensure that the buffer is completely homogenous and if any precipitate is visible, use gravity filtration to remove any precipitate immediately prior to use. See the note after step 3.3.1.

3.5.2. Using the UV/Vis spectrophotometer, blank the selected PBS buffer solution for a 200 - 800 nm range.

3.5.3. Into a second clean and dry quartz cuvette, transfer 1,900 µL of the selected PBS buffer then add 100 µL of the selected analog stock solution using a 5-50 µL micropipette. Place a cap on the cuvette and shake well in addition to inverting the cuvette.

NOTE: See the previous note after step 3.3.3.

3.5.4. Using the UV/Vis spectrophotometer, acquire the absorption spectrum for the dipyrrinone analog for a range of 200 – 800 nm.

3.5.5. Repeat steps 3.5.1 – 3.5.4 for **16** - **25** in each of the PBS buffers generated in step 3.2.

3.6. Determine the pK_a values for **16** – **25** using a best fit sigmoidal curve fitting function.

3.6.1. Using a graphing program, graph the measured absorbance vs. wavelength (nm) for **16** – **25** at the various pH levels.

3.6.2. Choose a wavelength between 380-415 nm where at lower pH levels (< 7.0) absorbance is small (0-0.1 units) and at greater pH (> 12.0) absorbance is considerably larger (0.8-1.0 units). Plot the absorbance at the chosen wavelength vs. the pH.

3.6.3. Using a sigmoidal curve function, generate a best fit curve for each of the analogs **16** – **25**. Report the extrapolated pH at half-height of the curve. This is the reported pK_a value.

4. Quantum Yield Acquisition and Fluorescence Studies

4.1. Create fluorescence study stock solutions for dipyrrinone analogs **16** – **18** and **20** – **25**.

4.1.1. Using a dipyrrinone analog stock solution created in step 3.1, perform a dilution of the stock solution by adding 10 µL of the stock solution to a 1 mL volumetric flask using a 2 - 20 µL micropipette, then add PBS (pH 7.0) buffer to the 1 mL mark. Place a cap on the volumetric flask and mix well by inverting and shaking the flask. This diluted stock solution will be used to generate the fluorescence spectra and will be referred to as the fluorescence stock solution.

4.1.2. Repeat step 4.1.1 for analogs **16** – **18** and **20** – **25**.

4.2. Acquire fluorescence emission spectra at varying concentrations, for analogs **16** – **18** and **20** – **25**. For all analogs other than **18**, acquire five spectra for each analog in solutions of pH 7 and 14 at concentrations of: 19.96, 39.84, 59.64, 79.37, and 99.01 nM. For analog 18, acquire five spectra in a solution of pH 7 at concentrations of: 49.75, 99.01, 147.8, 196.1, and 243.9 nM. In a solution of pH 14, acquire five spectra for analog 18 at concentrations of: 99.01, 196.1, 291.3, 384.6, 476.2 nM.

4.2.1. Into a transparent four-sided quartz cuvette, add 3.00 mL of PBS (pH 7.0) or 1.0 NaOH using a 100 -1,000 µL micropipette in three 1,000 µL increments.

NOTE: See note after step 3.3.1.

4.2.2. Using the fluorometer and the fluorometer software program FluorEssence, acquire an emission spectrum for the selected solution and label this as the solution "blank".

4.2.3. To the same cuvette, add 6 µL of fluorescence stock solution for the selected dipyrrinone analog (Part 4.1) using a 0.5-10 µL micropipette. Place the cap on the cuvette and mix well by inverting and gently shaking the cuvette.

NOTE: See note after step 3.3.3.

4.2.4. Using the fluorometer, acquire an emission spectrum for the selected compound solution using λ_{max} abs as the excitation wavelength. Excitation intensity was measured over a 200 nm range starting at 15 nm beyond the excitation wavelength (typically a 200 nm range is required for the fluorescence intensity to return to baseline).

4.2.5. Repeat steps 4.2.3 – 4.2.4 until a total of 30 µL of fluorescence stock solution has been added to the cuvette.

4.2.6. Repeat steps 4.2.1 – 4.2.5 for analogs **16** – **25** in PBS (pH 7.0) and 1.0 M NaOH.

NOTE: The cuvette concentrations were changed for analog **18** and data was acquired using: 2.0 mL of PBS with five consecutive 10 µL increments of fluorescence stock solution for a neutral (protonated **18**) solution and 2.0 mL of 1.0 M NaOH with five 20 µL increments of added compound stock solution for a basic (deprotonated **18**) solution.

4.3. Determine the quantum yield using the method of Williams, A. T. et al.[17]

4.3.1. Using a spreadsheet software program (i.e., Microsoft Excel), import the data (emission intensity data points) for the emission spectra for a single dipyrrinone analog (taken in either PBS [pH 7.0] or 1.0 M NaOH) at the various concentration levels.

4.3.2. Import the data points from the emission spectra for the "blank" solution (steps 4.2.1 – 4.2.2) and subtract the "blank" emission intensity data points from the emission intensity data points, at the corresponding wavelengths, acquired at various concentration levels.

4.3.3. Transfer the "blank" corrected emission intensity data points into a graphing program, such as GraphPad Prism 7, and plot emission vs. wavelength. Calculate the area under the curve for each of the curves obtained at the various concentration levels of dipyrrinone analog.

4.3.4. Following the technique outlined by Williams, A. T. et al, calculate an extrapolated absorbance value for each of the varying concentration levels of dipyrrinone analog. This is accomplished by multiplying the calculated molar absorptivity value (from best-fit linear regression analysis, see step 3.4) by each concentration of dipyrrinone analog used in steps 4.2.3-4.2.5.

4.3.5. Using a graphing program such as GraphPad Prism 7, create a plot of the analog's extrapolated absorbance (x-axis) against the calculated area under each concentration curve (step 4.3.4) for the emission wavelength corresponding to the greatest emission value. A linear relationship with a $r^2 \geq 0.96$ should be observed.

4.3.6. Perform steps analogous to 3.1-3.4 and 4.1-4.3.5 for quinine in 0.5 M H_2SO_4 ($\Phi_F = 0.55$)[18] and anthracene in ethanol ($\Phi_F = 0.27$)[18, 19] to obtain data for standards.

4.3.7. Obtain the quantum yield values for **16** - **25** in PBS (pH 7.0) and 1.0 M NaOH by using the extrapolated slopes obtained from steps 4.3.5 and 4.3.6 in the following equation:

$$\Phi_x = \Phi_{st}(Grad_x/Grad_{st})(\eta^2_x/\eta^2_{st})$$

where Φ_{st} represents the quantum yield of the standard, Φ_x represents the quantum yield of the unknown, *Grad* is the slope of the best linear fit, and η is the refractive index of the solvent used (the refractive index ratio was calculated using η = 1.36 for ethanol and η = 1.35 for 0.5 M H_2SO_4).

4.3.8. Report the quantum yields for **16** – **18** and **20** – **25** in PBS (pH 7.0) and 1.0 M NaOH as an average of the Φ_x obtained for quinine and anthracene.

REPRESENTATIVE RESULTS:

The Claisen-Schmidt condensation reaction provided access to dipyrrinone analogs (**16** – **25**, **Figure 4**) using the one-pot procedure described in the protocol section (see step 1). Analogs **16** – **25** were all generated by condensing pyrrolinone **9**, bromoisoindolone **10**, or isoindolone **11** with 1*H*-imidazole-2-carboxaldehyde (**12**), 1*H*-imidazole-5-carboxaldehyde (**13**), 1*H*-pyrazole-3-carboxaldehyde (**14**), or 1*H*-pyrazole-4-carboxaldehyde (**15**); the combinations produced ten different analogs including a control compound, **19**, which is incapable of forming intramolecular hydrogen bonds (**Table 1**). Reaction times typically necessitated 24 h of reflux for completion,

however, in the case of **20** only 6 h were required, whereas, for **23** and **24** slightly longer times of 30 h and 27 h respectively were needed. Product yields ranged from 41% to 96%, as illustrated in **Table 1**, which follow traditional trends of analogous condensation reactions for dipyrrinones. Compounds **17**, **18**, **20** – **22, 24** and **25,** due to their highly crystalline nature, were all purified by simple vacuum filtration methods; only compounds **16**, **19**, and **23** required chromatography for purification.

The photophysical properties of compounds **16** – **25**, obtained from performing steps 3 – 4 in the protocol section, are summarized in **Table 2**. The pK_a values measured for each compound ranged from 12 to > 13.5, suggesting sufficiently basic conditions are needed to completely deprotonate each dipyrrinone analog. Due to differing photophysical properties in the protonated and deprotonated states of each compound, spectra were acquired using neutral (pH 7.0 PBS) and basic (1.0 M NaOH) solutions of **16** – **25**. In neutral pH (protonated state), compounds **16** – **25** have λ_{max} abs ranging from 324 nm to 365 nm, which are all blue-shifted by 10 to 37 nm in comparison to the deprotonated states. The molar absorptivities range from 15,000 to 30,000 but do not appear to substantially deviate amongst the protonated and deprotonated states of a given analog. Analog **19** did not display any detectable fluorescence, however, **16** – **18** and **20** – **25** emitted light with λ_{max} em ranging from 409 – 457 nm at neutral pH and 443 – 482 nm at basic pH; a similar red-shifting trend to that of the maximum protonated/deprotonated absorbance wavelengths is observed for the emission wavelengths as well. The Φ_F ranged from 0.01 to 0.30 in both neutral and basic aqueous solutions, which are considerably lower than comparable xanthoglows, but compounds **16**, **20**, and **25** fall in the similar region of heavily used fluorophores such as rhodamine B (Φ_F = 0.23),[20] acridine orange (Φ_F = 0.36),[21] pyronin Y (Φ_F = 0.22),[20] and most of the cyanine dye series (typically Φ_F = 0.12-0.28).[22]

Dipyrrinone analogs **16** – **25** were all chemically characterized using melting point analysis, IR spectroscopy, ^{1}H NMR and ^{13}C NMR spectroscopy, and high-resolution mass spectrometry in addition to the UV/Vis and fluorescence spectroscopy experiments summarized in Table 2. Chemical characterization and original ^{1}H NMR and ^{13}C NMR spectra can be found from the original literature source,[12] however, for convenience, characterization for compounds **16**, **20**, and **23**, which possess the largest quantum yields are reported below:

(Z)-5-((1H-imidazol-2-yl)methylene)-3-ethyl-4-methyl-1,5-dihydro-2H-pyrrol-2-one (16). Decomposes at 160 °C; ^{1}H NMR (400 MHz, DMSO-d6) δ 12.3 (brs, 1H), 9.87 (s, 1H), 7.13 (apps, 2H), 5.93 (s, 1H), 2.23 (q, J = 7.5 Hz, 2H), 2.00 (s, 3H), 0.98 (t, J = 7.5 Hz, 3H); ^{13}C NMR (101 MHz, DMSO- d6) δ 170.7, 144.8, 140.0, 139.6, 133.9, 130.2, 117.6, 94.1, 16.7, 13.6, 9.33; IR (thin film) 3742, 3148, 3063, 2924, 2353, 1651, 1543, 1450, 771, 717 cm^{-1}; HRMS (ESI-TOF) m/z: $[M+Na]^+$ Calcd for $C_{11}H_{13}N_3ONa$ 226.0956, Found 226.0956.

(Z)-5-((1H-pyrazol-4-yl)methylene)-3-ethyl-4-methyl-1,5-dihydro-2H-pyrrol-2-one (19). Decomposes at 202 ºC; ^{1}H NMR (400 MHz, 20% CD_3OD in $CDCl_3$) δ ^{1}H NMR (400 MHz, Chloroform-*d*) δ 7.74 (s, 2H), 6.01 (s, 1H), 2.27 (q, *J* = 7.4 Hz, 2H), 2.02 (s, 3H), 1.02 (t, *J* = 7.4 Hz, 3H); ^{13}C{^{1}H} NMR (101 MHz, $CDCl_3$) δ 173.7, 141.9, 136.0, 133.0, 116.1, 105.0, 100.8, 16.9, 13.4, 9.61; IR (thin film) 3163, 3117, 3048, 2963, 2362, 1674, 1558, 1512, 1396, 1257, 1157, 948, 871, 794, 702 cm^{-}

436 [1]; HRMS (ESI-TOF) *m/z*: $[M+Na]^+$ Calcd for $C_{11}H_{13}N_3ONa$ 226.0956, Found 226.0955.
437
438 **(Z)-3-((1H-imidazol-2-yl)methylene)-5-bromoisoindolin1-one (20).** Decomposes at 213 °C; ^1H
439 NMR (400 MHz, DMSO-d6) δ 7.97 (s, 1H), 7.59 (d, J = 7.8 Hz, 1H), 7.48 (d, J = 8.0, 1H), 7.06 (s, 2H),
440 6.57 (s, 1H); ^{13}C NMR (101 MHz, DMSO-d6) δ 167.7, 146.6, 140.2, 134.5, 131.7, 129.1, 125.8,
441 125.03, 124.99, 123.6, 96.5; IR (thin film) 3742, 3240, 2314, 1682, 1543, 1520, 1435, 1312, 1080,
442 826, 694 cm^{-1}; HRMS (ESI-TOF) m/z: $[M+Na]^+$ Calcd for $C_{12}H_8BrN_3ONa$ 311.9749, Found 311.9752.
443
444 **(Z)-3-((1H-imidazol-2-yl)methylene)isoindolin-1-one (23).** Decomposes at 228 °C; ^1H NMR (400
445 MHz, DMSO-d6) δ 12.34 (s, 1H), 10.74 (s, 1H), 7.90 (d, J = 7.5 Hz, 1H), 7.74 (d, J = 7.6 Hz, 1H), 7.63
446 (dd, J = 7.6, 7.2 Hz, 1H), 7.50 (dd, J = 7.6, 7.3 Hz, 1H), 7.17 (s, 2H), 6.46 (s, 1H); ^{13}C NMR (101 MHz,
447 DMSO-d6) δ 167.3, 144.9, 137.3, 135.1, 132.8, 129.9, 129.3, 123.6, 121.0, 117.6, 92.9; IR (thin
448 film) 3741, 3201, 3086, 2361, 2322, 1682, 1543, 1520, 1119, 748, 687 cm^{-1}; HRMS (ESI-TOF) m/z:
449 $[M+Na]^+$ Calcd for $C_{12}H_9N_3ONa$ 234.0643, Found 234.0641.
450
451 **Table 1.** Conditions and reaction yields for the synthesis of **16**-**25**[a]
452 [a] Reactions performed on a 1 mmol scale in 5 mL of EtOH. [b] Isolated Yield.
453
454 **Table 2.** Photophysical properties and pKa values of **6**-**14** and **22** in pH 7.0 PBS buffer and 1 M
455 NaOH (given in parenthesis).
456 [a] Fluorescence was not detectable for **19**. [b] Quinine (Q = 0.55)[15] and Anthracene (Q = 0.27)[15, 16]
457 were used as standards.
458
459 **DISCUSSION:**
460 The Claisen-Schmidt condensation approach provides a fairly robust means of generating
461 pyrazole, imidazole, and isoindolone dipyrrinone fluorophores through a relatively operationally
462 simplistic protocol. While the synthesis of the fluorescent dipyrrinone analogs was the focus of
463 this study, it should be noted that similar conditions can be applied to access other bicyclic
464 methine-linked ring systems such as dipyrrinones[23-25] and pyrrole-furan adducts[26] as well as 3H-
465 pyrazol-3-one-furan adducts[27], isoindolone pyrrole adducts[28], and 2*H*-Indol-2-one-pyrindine
466 adducts[29] which hold promise as potential pharmaceuticals. In general, the described procedure
467 provides reaction products in moderate to high yields, however, it is important to note that
468 continual monitoring of the reaction progress is essential for successful outcomes. In some of our
469 preliminary trials, it was found that heating for excessive reaction times, well beyond (5 – 24 h)
470 the completion of the reaction, led to decomposition products which can complicate the
471 subsequent purification steps. For this reason, it is highly recommended that TLC analysis is
472 performed at 1 h, 3 h, 6 h, 12 h, and 24 h time marks to monitor the reaction progress and to
473 gain a sense of the reaction rate, as well as the rate of product decomposition.
474
475 Dipyrrinone analogs **16** – **25**, in the protonated/neutral state, possess a range of solubility
476 properties in commonly used organic solvents which can be problematic when studying
477 photophysical, biological, and analytical properties. In general, **16** – **25** had varied solubility in
478 water, alcohol solvents (methanol/ethanol), and CH_2Cl_2 but all had good solubility in highly polar
479 aprotic solvents such as DMF, DMSO, and acetonitrile. Consequently, all stock solutions for

UV/Vis (Step 3.1 of protocol) and fluorescence studies (Step 4.1 of protocol) and most NMR studies were carried out using DMSO or DMSO-d6. Though most compounds required gentle heating (using a heat gun) to completely solubilize in DMSO, once dissolved, **16** – **25** appear to remain soluble and can even be diluted in aqueous solutions without precipitating. Due to the highly polar nature of the ionic state, analogs **16** – **25** in basic solution are highly water soluble but have little solubility in organic solvents.

While the Claisen-Schmidt condensation reaction provides access to a range of methine-linked bicyclic aromatic compounds, beyond the dipyrrinone analogs describe within, the reaction conditions can limit the types of molecules produced through this method. As a fundamental requirement of the reaction, both an enolizable nucleophile (such as a pyrrolinone or isoindolone) and a non-enolizable aldehyde electrophile must react to enable the condensation. Failure to meet this basic requirement may result in the inability to link together the ring systems and/or the generation of competing side products. In addition, considerably basic conditions are used for generating the enolate nucleophile, which can create incompatibilities with functional groups (i.e., esters, nitriles, halides, etc.) that are susceptible to reactions with hydroxide. In such cases, it is possible to substitute hydroxide with nitrogenous bases or carbonate, as has been accomplished with 1,8-Diazabicyclo[5.4.0]undec-7-ene (DBU)[30], triethylamine[31], piperidine[32], Hünig's base[33], and Na_2CO_3[34]. In order to carry out an analogous reaction, we chose to use sodium hydroxide simply due to its availability and relative expense. While these constraints may require modifications to the procedure to access specific compounds or prevent access to others altogether, the method outlined in the protocol can provide a means of coupling aromatic rings for numerous systems through a procedurally simple and cost-effective single step reaction. In the case of dipyrrinone analogs **16** – **25**, the Claisen-Schmidt condensation has enabled one of the most accessible routes to pH dependent fluorophores described to date.

The Claisen-Schmidt condensation reaction has the potential to serve as a key reaction for the creation of a range of different bicyclic and tricyclic fluorophore systems. While this reaction has been critical to the development of 3H,5H-dipyrrolo[1,2-c:2',1'-f]pyrimidin-3-ones (**1**), xanthoglows (**2**), pyrroloindolizinedione analogs (**3**, **Figure 1**), and most recently dipyrrinone analogs **16** – **25**, it is possible to generate a range of completely novel fluorescent systems through pairing the Claisen-Schmidt condensation with molecular designs to restrict photoisomeric processes. More specific to the study at hand, future designs of dipyrrinone analogs will likely be developed using this outlined procedure in order to generate fluorescent compounds with stronger intramolecular hydrogen bonding capacity and lower pK_a values. We anticipate these enhanced pH dependent probes will possess higher quantum yields while enabling the visualization of pH fluctuations for a wider range of intracellular events.

ACKNOWLEDGMENTS:

Z.R.W. and N.B. thank the NIH (2P20 GM103440-14A1) for their generous funding as well as Jungjae Koh and the University of Nevada, Las Vegas for their assistance in acquiring ^{1}H and ^{13}C NMR. Additionally, we would like to thank NSC visual media students, Arnold Placencia-Flores and Alistair Cooper for their help in the filming and animation processes within the cinematography portions of this manuscript.

DISCLOSURES:

The authors have nothing to disclose.

REFERENCES:

1. Abbandonato, G. et al. Cis-trans photoisomerization properties of GFP chromophore analogs. *European Biophysics Journal*. **40** (11), 1205-1214 (2011).
2. Funakoshi, H. et al. Spectroscopic studies on merocyanine photoisomers. IV. Catalytic isomerization of photoisomers of merocyanine derivatives in protic solvents. *Nippon Kagaku Kaishi*. (9), 1516-22 (1989).
3. Puzicha, G., Shrout, D. P., Lightner, D. A. Synthesis and properties of homomologated and contracted dipyrrinone analogs of xanthobilirubic acid. *Journal of Heterocyclic Chemistry*. **27** (7), 2117-23 (1990).
4. Bonnett, R., Hamzetash, D., Asuncion Valles, M. Propentdyopents [5-(2-oxo-2H-pyrrol-5-ylmethylene)pyrrol-2(5H)-ones] and related compounds. Part 2. The Z ⇆ E photoisomerization of pyrromethenone systems. *Journal of the Chemical Society, Perkins Transactions*. **1** (6), 1383-8 (1987).
5. Tikhomirova, K., Anisimov, A., Khoroshutin, A. Biscyclohexane-Annulated Diethyl Dipyrrindicarboxylates: Observation of a Dipyrrin Form with Absent Visible Absorption. *European Journal of Organic Chemistry*. **2012** (11), 2201-2207, S2201/1-S2201/8 (2012).
6. Brower, J. O., Lightner, D. A. Synthesis and spectroscopic properties of a new class of strongly fluorescent dipyrrinones. *Journal of Organic Chemistry*. **67** (8), 2713-2716 (2002).
7. Woydziak, Z. R., Boiadjiev, S. E., Norona, W. S., McDonagh, A. F., Lightner, D. A. Synthesis and Hepatic Transport of Strongly Fluorescent Cholephilic Dipyrrinones. *Journal of Organic Chemistry*. **70** (21), 8417-8423 (2005).
8. Jarvis, T. et al. Pyrrole β-amides: Synthesis and characterization of a dipyrrinone carboxylic acid and an N-Confused fluorescent dipyrrinone. *Tetrahedron*. **74** (14), 1698-1704 (2018).
9. Bodio, E., Denat, F., Goze, C. BODIPYS and aza-BODIPY derivatives as promising fluorophores for in vivo molecular imaging and theranostic applications. *Journal of Porphyrins and Phthalocyanines*. **23** (11/12), 1159-1183 (2019).
10. Acharya, A. et al. Photoinduced Chemistry in Fluorescent Proteins: Curse or Blessing? *Chemical Reviews*. **117** (2), 758-795 (2017).
11. Romei, M. G., Lin, C.-Y., Mathews, I. I., Boxer, S. G. Electrostatic control of photoisomerization pathways in proteins. *Science*. **367** (6473), 76-79 (2020).
12. Benson, N., Suleiman, O., Odoh, S. O., Woydziak, Z. R. yrazole, Imidazole, and Isoindolone Dipyrrinone Analogues: pH-Dependent Fluorophores That Red-Shift Emission Frequencies in a Basic Solution. *Journal of Organic Chemistry*. **84** (18), 11856-11862 (2019).
13. Xie, P., Gao, G., Liu, J., Jin, Q., Yang, G. A New Turn on Fluorescent Probe for Selective Detection of Cysteine/Homocysteine. *Journal of Fluorescence*. **25** (5), 1315-1321 (2015).
14. Alty, I. G. et al. Intramolecular Hydrogen-Bonding Effects on the Fluorescence of PRODAN Derivatives. *Journal of Physical Chemistry A*. **120** (20), 3518-3523 (2016).
15. Yang, Y., Li, D., Li, C., Liu, Y. F., Jiang, K. Hydrogen bond strengthening induces fluorescence quenching of PRODAN derivative by turning on twisted intramolecular charge transfer.

Spectrochimica Acta, Part A. **187**, 68-74 (2017).
16. Zhang, L., Liu, J., Gao, J., Zhang, F., Ding, L. High solid fluorescence of a pyrazoline derivative through hydrogen bonding. *Molecules*. **22** (8), 1304/1-1304/7 (2017).
17. Williams, A. T. R., Winfield, S. A., Miller, J. N. Relative fluorescence quantum yields using a computer-controlled luminescence spectrometer. *Analyst*. **108** (1290), 1067-71 (1983).
18. Eaton, D. F. Reference materials for fluorescence measurement. *Pure and Applied Chemistry*. **60** (7), 1107-14 (1988).
19. Dawson, W. R., Windsor, M. W. Fluorescence yields of aromatic compounds. *Journal of Physical Chemistry*. **72** (9), 3251-60 (1968).
20. Zhang, X.-F., Zhang, J., Lu, X. The Fluorescence Properties of Three Rhodamine Dye Analogues: Acridine Red, Pyronin Y and Pyronin B. *Journal of Fluorescence*. **25** (4), 1151-1158 (2015).
21. Zanker, V., Rammensee, H., Haibach, T. Measurements of the relative quantum yields of the fluorescence of acridine and fluorescein dyes. *Zeitschrift für Angewandte Physik*. **10**, 357-361 (1958).
22. Mujumdar, R. B., Ernst, L. A., Mujumdar, S. R., Lewis, C. J., Waggoner, A. S. Cyanine dye labeling reagents: Sulfoindocyanine succinimidyl esters. *Bioconjugate Chemistry*. **4** (2), 105-111 (1993).
23. Battersby, A. R., Dutton, C. J., Fookes, C. J. R. Synthetic studies relevant to biosynthetic research on vitamin B12. Part 7. Synthesis of (±)-bonellin dimethyl ester. *Journal of the Chemical Society, Perkin Transactions*. **1** (6), 1569-76 (1988).
24. Pfeiffer, W. P., Lightner, D. A. (m.n)-Homorubins: syntheses and structures. *Monatschfte für Chemie*. **145** (11), 1777-1801 (2014).
25. Huggins, M. T., Musto, C., Munro, L., Catalano, V. J. Molecular recognition studies with a simple dipyrrinone. *Tetrahedron*. **63** (52), 12994-12999 (2007).
26. Groselj, U. et al. Synthesis of Spiro-δ2-Pyrrolin-4-One Pseudo Enantiomers via an Organocatalyzed Sulfa-Michael/Aldol Domino Sequence. *Advanced Synthesis & Catalyst*. **361** (22), 5118-5126 (2019).
27. El-Shwiniy, W. H., Shehab, W. S., Mohamed, S. F., Ibrahium, H. G. Synthesis and cytotoxic evaluation of some substituted pyrazole zirconium(IV) complexes and their biological assay. *Applied Organometallic Chemistry*. **32** (10) (2018).
28. Murray, L., O'Farrell, A.-M., Abrams, T. Preparation of indolinone compounds for treatment of excessive osteolysis. US20040209937A1, US Patent (2004).
29. Lozinskaya, N. A. et al. Synthesis and biological evaluation of 3-substituted 2-oxindole derivatives as new glycogen synthase kinase 3β inhibitors. *Bioorganic & Medicinal Chemistry*. **27** (9), 1804-1817 (2019).
30. Montforts, F. P., Schwartz, U. M. A directed synthesis of the chlorin system. *Liebigs Annalen der Chemie*. (6), 1228-53 (1985).
31. Uddin, M. I., Thirumalairajan, S., Crawford, S. M., Cameron, T. S., Thompson, A. Improved synthetic route to C-ring ester-functionalized prodigiosenes. *Synlett*. (17), 2561-2564 (2010).
32. Brower, J. O., Lightner, D. A., McDonagh, A. F. Aromatic congeners of bilirubin: synthesis, stereochemistry, glucuronidation and hepatic transport. *Tetrahedron*. **57** (37), 7813-7827 (2001).
33. Clift, M. D., Thomson, R. J. Development of a Merged Conjugate Addition/Oxidative Coupling Sequence. Application to the Enantioselective Total Synthesis of Metacycloprodigiosin

and Prodigiosin R1. *Journal of the American Chemical Society*. **131** (40), 14579-14583 (2009).
34. Brower, J. O., Lightner, D. A., McDonagh, A. F. Synthesis of a New Lipophilic Bilirubin. Conformation, Transhepatic Transport and Glucuronidation. *Tetrahedron*. **56** (40), 7869-7883 (2000).

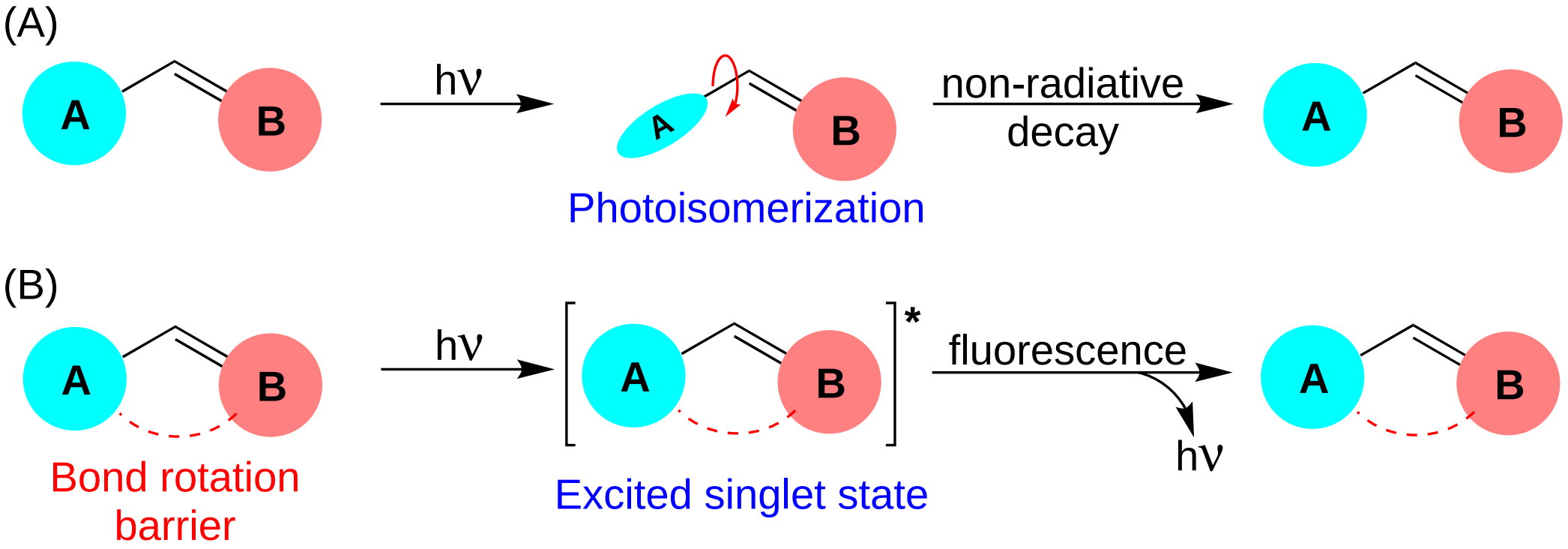

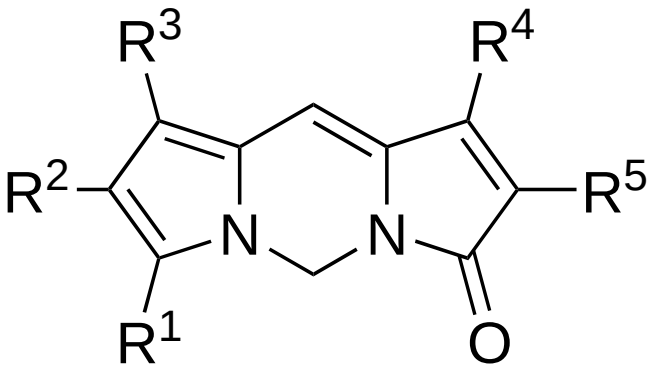

1

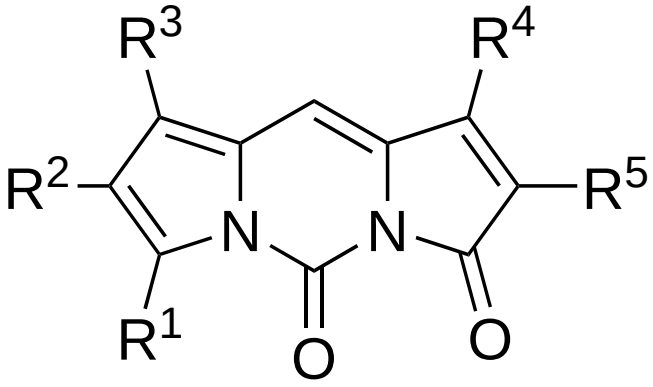

2

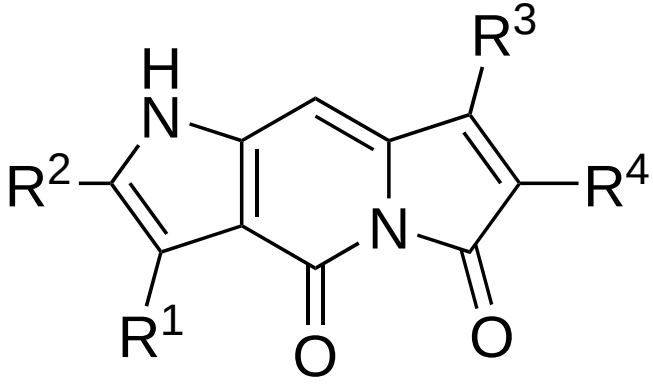

3

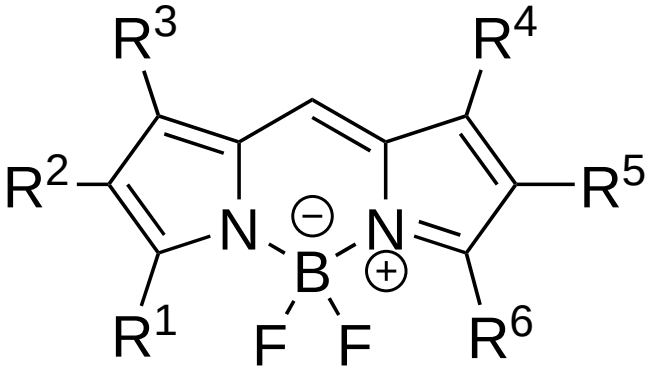

4

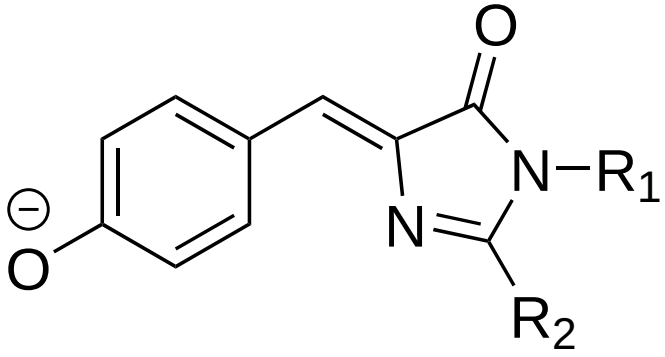

5

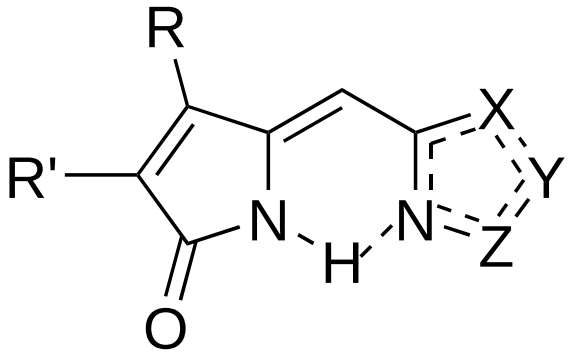

6: X=NH, Y/Z=CH
7: Y=NH, X/Z=CH
8: Z=NH, X/Y=CH

Figure

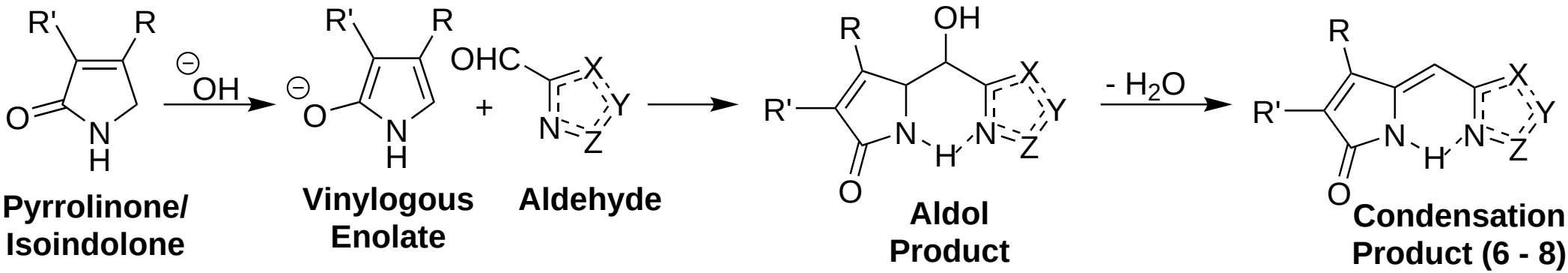

Figure

Click here to access/download;Figure;Figure 4.eps

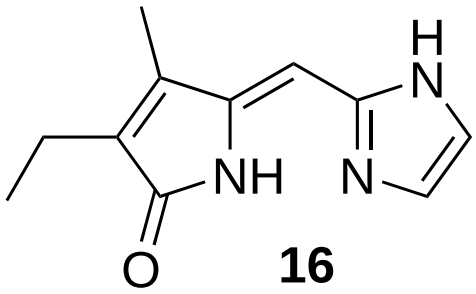

16

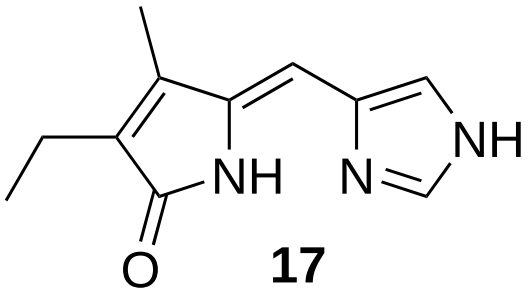

17

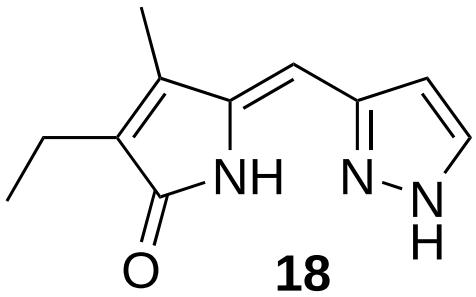

18

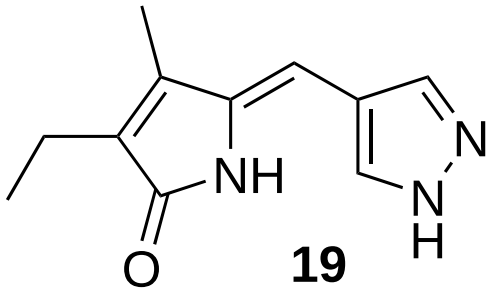

19

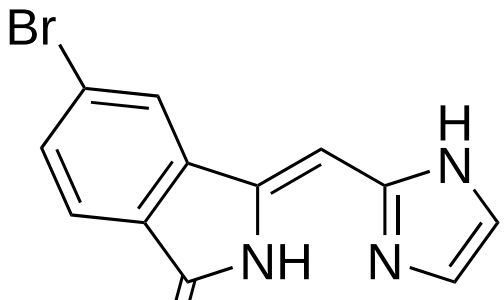

20

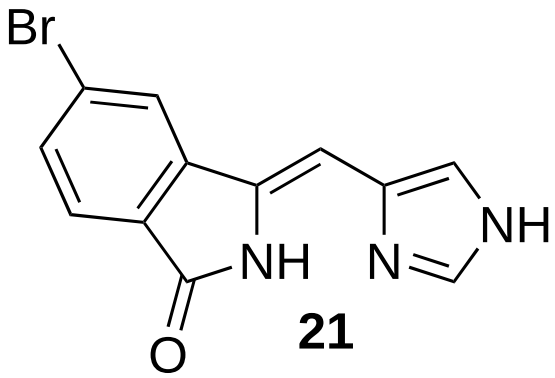

21

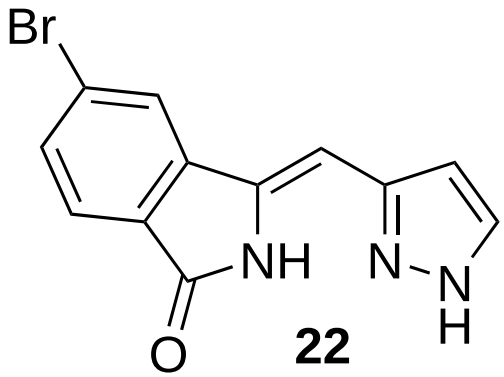

22

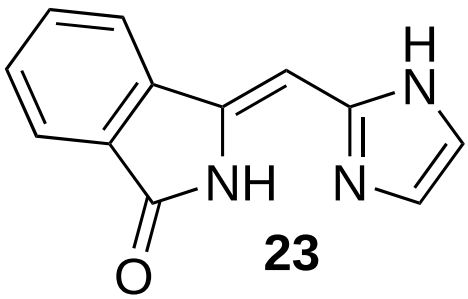

23

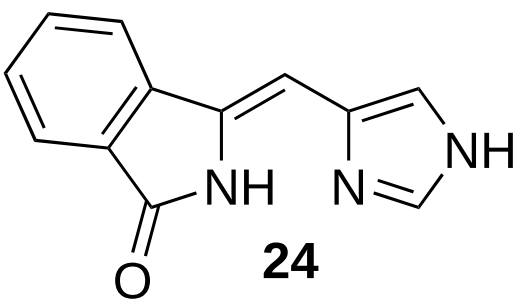

24

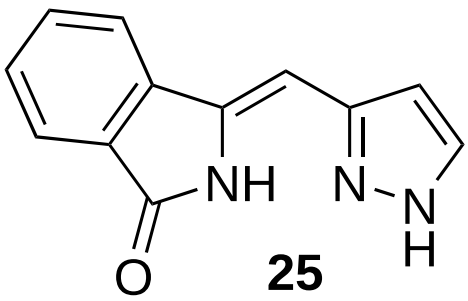

25

Table

Entry	Pyrrolinone/Isoindolone	Aldehyde	Yield (%)[b]	Time (h)	Product
1	**9**	**12**	80	24	**16**
2	**9**	**13**	41	24	**17**
3	**9**	**14**	79	24	**18**
4	**9**	**15**	61	24	**19**
5	**10**	**12**	96	6	**20**
6	**10**	**13**	70	24	**21**
7	**10**	**14**	66	24	**22**
8	**11**	**12**	49	30	**23**
9	**11**	**13**	49	27	**24**
10	**11**	**14**	94	24	**25**

Table

Compound	Abs. λ_{max} (nm)	ε (M^{-1} cm^{-1})	Fluor. λ_{max} (nm)	Φ^b	pK_a
16	351 (384)	24500 (22800)	451 (482)	0.30 (0.30)	12.7
17	338 (380)	18600 (18600)	442 (462)	0.01 (0.03)	12.8
18	324 (349)	29800 (25700)	455 (465)	0.01 (0.02)	13
19	326 (358)	29900 (21300)	–[a]	–[a]	12.9
20	365 (378)	15000 (15500)	457 (475)	0.22 (0.20)	12.5
21	355 (380)	15100 (16800)	409 (443)	0.03 (0.01)	12.9
22	341 (363)	19800 (23100)	427 (452)	0.02 (0.01)	>13.5
23	360 (373)	29000 (21300)	449 (474)	0.25 (0.26)	12
24	351 (373)	17200 (19400)	432 (454)	0.07 (0.05)	12.8
25	340 (357)	20200 (23500)	410 (449)	0.02 (0.02)	>13.5

Name of Material/ Equipment	Company	Catalog Number[a]	nents/Description
3-ethyl-4-methyl-3-pyrrolin-2-one	Combi-Blocks	[766-36-9]	ow solid reagent
isoindolin-1-one	ArkPharm	[480-91-1]	/hite solid reagent
5-bromoisoindolin-1-one	Combi-Blocks	[552330-86-6]	ık solid reagent
2-formylimidazole	Combi-Blocks	[10111-08-7]	/hite solid reagent
Imidazole-4-carbaldehyde	ArkPharm	[3034-50-2]	Solid reagent
1-H-pyrazole-4-carbaldehyde	Oakwood Chemicals	[35344-95-7]	Solid reagent
1-H-pyrazole-5-carbaldehyde	Matrix Scientific	[3920-50-1]	Solid reagent
Solid KOH Pellets	BeanTown Chemicals	[1310-58-3]	ıite solid pellets
Siliflash Silica Gel	Scilicycle	R12030B	e white powder
Phosphate Buffered Saline (PBS) (x10)	Growcells	MRGF-6235	ss translucent liquid
Beckman Coulter DU-800 UV/Vis Spectrophotometer and Software	Beckman Coulter	N/A	' Instrument and Software
Fluoromax-4 Spectrofluorometer	Horiba Scientific	N/A	·oscopy Instrument

FluorEssence Fluorometry Software V3.5	Horiba Scientific	N/A	troscopy Software
Finnpipette II Micropipette (sizes: 100-1,000, 20-200, and 0.5-10 µL)	Fischerbrand	N/A	Equipment
Wilmad-LabGlass Rotary Evaporator (Model: WG-EV311-V-PLUS)	SP Sciencewar e	N/A	Equipment
DuoSeal Vacuum Pump (Model Number: 1405)	Welch	N/A	Equipment
GraphPad Prism 4	GraphPad	N/A	Analysis Software
SympHony pH Meter (Model: Sb70P)	VWR	N/A	Equipment

NEVADA STATE COLLEGE

Zachary R. Woydziak, Ph.D.
Associate Professor of Chemistry
Nevada State College
1300 Nevada State Dr,
Henderson, NV 89002
(702)-992-2656
zachary.woydziak@nsc.edu

Febuary 23, 2021

Dr. Nam Nguyen
Manager of Review
Journal of Visualized Experiments

Dear Dr. Nguyen,

We are happy to resubmit our manuscript "Synthesis of pH Dependent Pyrazole, Imidazole, and Isoindolone Dipyrrinone Fluorophores Using a Claisen-Schmidt Condensation Approach" to the Journal of Visualized Experiments. We very much appreciate the additional recommendations of the editors who have made most helpful suggestions to help us shape this draft. Below is a point-by-point response to the changes/suggestions requested by the editorial team and the reviewers.

As your editorial team has requested, we have edited our manuscript to include the following modifications to the manuscript portion (in red below):

1. We spelled out all journal titles.

Additionally, we made the following edits (in red) to the movie file as your editorial teams suggested:

1. Pacing

Instead of using the dip to black, I highly recommend dipping to white instead, because that's the background color behind the talent. Dipping to black is too jarring in contrast. I've highlighted all the times this change needs to occur: 00:54, 01:41, 03:23, 04:04, 13:17 – We modified the video as recommended.

04:21 - 04:21 All these shots need to be cross dissolved together instead of the straight cuts in order to show a smoother sequence. – We modified the video as recommended.

08:51 - 08:59 We don't need to see the funnel being placed on the holder after its been shaken. There's too much of a silent gap here. Use a cross dissolve to the next shot please. – We modified the video as recommended.

NEVADA STATE
COLLEGE

09:28 - 09:32 Tighten this up please. There's a gap with no narration. Then suddenly the shot cuts to the next step but the narration doesn't start for another two seconds. – We modified the video as recommended.

09:38 - 09:38 The cut happens too soon. I'd like to see more of the rotary evaporator. It shouldn't cut to this next shot until the narration starts. – We modified the video as recommended.

14:14 - 14:14 I didn't catch this last time, but I would fade out sooner. It looks awkward to see him starting to lean at the end. – We modified the video as recommended.

Thank you for your consideration.

Sincerely,

Zachary Woydziak

Zachary R. Woydziak, Ph.D.

1300 Nevada State Drive • Henderson, NV 89015 • 702.992.2000 • fax 702.992.2226
www.nsc.nevada.edu